Electronic Supplementary Information

Reductively convertible nickel phthalocyanine precursor as a biological thiol-responsive turn-on photoacoustic agent

Kohei Nogita,[a] Takaya Sugahara,[a] Koji Miki,*[a] Huiying Mu,[a] Minoru Kobayashi,[b] Hiroshi Harada,[b] and Kouichi Ohe*[a]

[a] Department of Energy and Hydrocarbon Chemistry,
Graduate School of Engineering, Kyoto University,
Katsura, Nishikyo-ku, Kyoto 615-8510, Japan.
E-mail: kojimiki@scl.kyoto-u.ac.jp; ohe@scl.kyoto-u.ac.jp
[b] Laboratory of Cancer Cell Biology,
Graduate School of Biostudies, Kyoto University,
Yoshida, Sakyo-ku, Kyoto 606-8501, Japan.

Index

1. Experimental section

1.1. Materials and methods

1-Ethyl-(3-(dimethylamino)propyl)carbodiimide hydrochloride (EDC·HCl) was purchased from Watanabe Chemical Industries, Ltd. (Japan). Triethylamine, ethylene glycol, 4-dimethylaminopyridine (DMAP), dichloromethane (CH_2Cl_2), Dulbecco's modified Eagle's medium (DMEM), and 1% penicillin/streptomycin (P/S) were purchased from Fujifilm-Wako Pure Chemicals Industries, Ltd. (Japan). Methylene blue was purchased from Waldeck GmbH & Co. KG (Germany). (3-(4,5-dimethylthiazol-2-yl)-2,5-diphenyltetrazolium bromide (MTT), glycine (Gly), alanine (Ala), valine (Val), lysine (Lys), and phosphate buffer solution (pH 7.2, 0.1 M) were purchased from Tokyo Chemical Industry Co., Ltd. (Japan). Nickel acetate tetrahydrate, dimethyl sulfoxide (DMSO), *N*-ethylmaleimide (NEM), tyrosine (Tyr), histidine (His), serine (Ser), threonine (Thr), methionine (Met), glutamine (Gln), glutamic acid (Glu), cysteine (Cys), glutathione (GSH, reduced), and methanol (MeOH) were purchased from nacalai tesque (Japan). $MgSO_4$ was purchased from Kishida Chemical Co., Ltd. (Japan). Phthalonitrile and homocysteine (Hcy) were purchased from Aldrich Chemical Co. (USA). Isoflurane was purchased from Viatris Inc. (USA). Silica gel (SiO_2, 230–400 mesh) for column chromatography was purchased from Silicycle (Canada).

PEG-COOH was prepared from poly(ethylene glycol) monomethyl ether (MW = 2000) according to the reported method.[1]

Buffered solutions (pH 5.8–8.0) were prepared by dissolving sodium dihydrogenphosphate (NaH_2PO_4) and disodium hydrogenphosphate (Na_2HPO_4) in water (MilliQ).

UV-vis absorption spectra were recorded by UV-vis spectrophotometer (UH5300, Hitachi High Technologies, Japan).

PA signals were measured by Nexus 128 (ENDRA Life Sciences Inc., USA). The sample solutions were kept in dark at room temperature for more than 3 h before measurement.

Mass spectra were measured by Exactive Plus Orbitrap (ESI, Thermo Fisher Scientific Inc., USA) and Ultraflex III (MALDI, Bruker Co., USA).

IR absorption spectra were measured by Spectrum Two (FT-IR, PerkinElmer Inc., USA).

1.2. Synthesis

1.2.1 Synthesis of ox-NiPc-OH

In a 100 mL two-necked round-bottom flask, phthalonitrile (0.22 g, 1.8 mmol), nickel acetate tetrahydrate (0.11 g, 0.43 mmol), and triethylamine (0.50 mL, 3.6 mmol) in ethylene glycol (2 mL) were stirred at 55 °C under nitrogen atmosphere. After stirring for 12 h, the dark-green suspension was diluted with CH_2Cl_2 (30 mL) and filtered to remove the blue solid. The resulting red crude solution was washed with H_2O (30 mL × 3) and the organic layer was dried over $MgSO_4$. After the organic solvent was removed under reduced pressure, the crude product was purified by column chromatography on SiO_2 (eluent: CH_2Cl_2/MeOH, v:v = 1:0 to 0:1) to afford **ox-NiPc-OH** (0.11 g, 0.16 mmol, 38%) as a reddish-brown solid. When triethylamine was not added to the reaction solution, the isolated yield was 11% even after the reaction for 24 h.

ox-NiPc-OH: IR (neat) 3323, 3061, 2934, 2871, 1640, 1614, 1568, 1535, 1488, 1455, 1407, 1326, 1292, 1248, 1195, 1166, 1148, 1128, 1093, 1064, 1035, 1004, 957, 923, 884, 845, 773, 727, 678, 659, 623, 603, 589, 581, 567, 542, 533, 525, 513 cm^{-1}; ^1H NMR (400 MHz, $CDCl_3$, 25 °C) δ = 3.36–3.46 (m, 2H), 3.80–3.90 (m, 6H), 7.51–7.58 (m, 6H), 7.60–7.64 (m, 2H), 7.85–7.87 (m, 4H), 7.96–7.99 (m, 4H). ^{13}C NMR (100 MHz, $CDCl_3$, 25 °C) δ = 61.7, 65.7, 100.4, 122.0, 122.3, 122.7, 123.3, 130.0, 131.7, 131.8, 135.7, 138.1, 147.0, 161.6, 165.2, 168.1. HRMS (ESI) calcd for $C_{36}H_{26}N_8NaO_4$ ($[M+Na]^+$) 715.1323, found 715.1324.

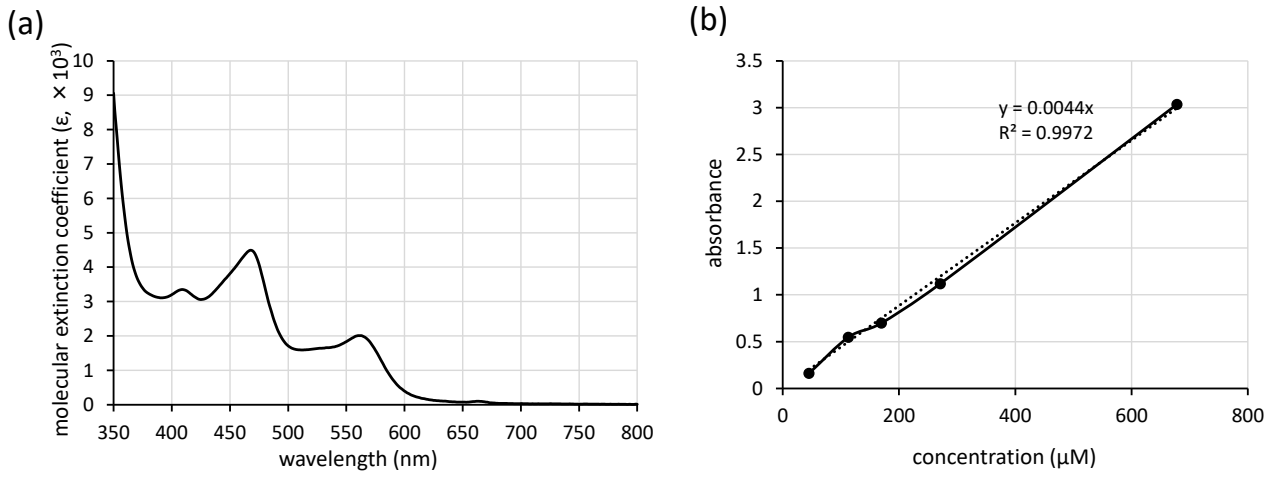

Fig. S1 (a) UV-vis absorption spectrum of **ox-NiPc-OH** in $CHCl_3$. (b) Absorbance of **ox-NiPc-OH** in $CHCl_3$ at 468 nm.

1.2.2. Synthesis of ox-NiPc-PEG

In a 50 mL Schlenk tube, EDC·HCl (0.18 g, 0.91 mmol), DMAP (0.15 mg, 1.2 μmol), **PEG-COOH** (1.1 g, 0.51 mmol), and CH_2Cl_2 (3.0 mL) were stirred at room temperature for 20 min. After addition of **ox-NiPc-OH** (0.10 g, 0.15 mmol), the solution was stirred at room temperature for 6 h. The resulting solution was washed with H_2O (50 mL × 3) and the organic solvent was removed under reduced pressure. The crude red solid was dissolved in water. The aqueous solution was filtered to remove unreacted **ox-NiPc-OH**. The filtrate was freeze-dried and **ox-NiPc-PEG** (45%, containing a small amount of free **PEG-COOH**) as a red solid was obtained. In MALDI-TOF mass spectrum of **ox-NiPc-PEG**, the fragment peaks of ox-NiPc bearing one PEG chain and peaks of PEG fragments were observed together with the parent peaks (Fig. S2).

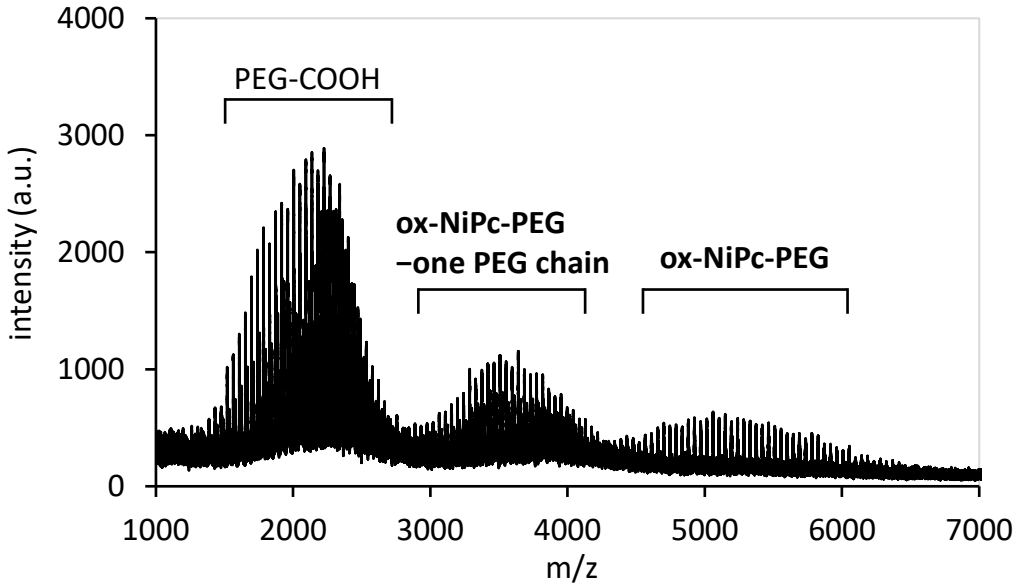

Fig. S2 MALDI-TOF mass spectrum of **ox-NiPc-PEG**. Matrix: dithranol.

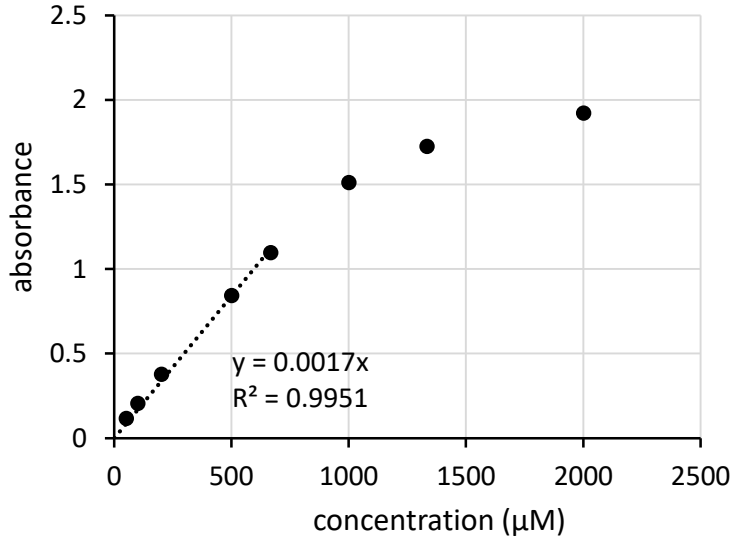

Fig. S3 Absorbance of **ox-NiPc-PEG** in water at 459 nm.

1.3. Theoretical calculation

The density functional theory (DFT) calculations were performed for the geometry optimization of two isomers of **ox-NiPc-OH** having two hydroxyethoxy groups at the B3LYP/LANL2DZ level for Ni and the B3LYP/6-31G(d, p) level for C, H, N, O by using Gaussian 16 package.[2,3] Their electronic and Gibbs free energies are summarized in Table S1. The cartesian coordinates of the optimized structures are summarized at the end of the ESI.

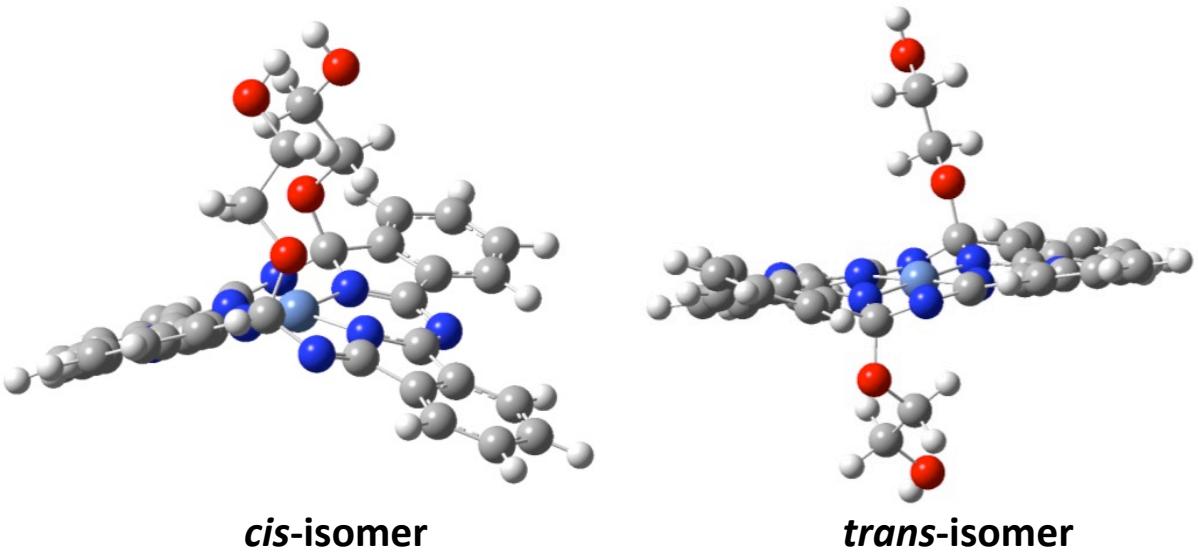

Fig. S4 Energy-minimized structures of two isomers at the B3LYP/LANL2DZ level for Ni and the B3LYP/6-31G (d, p) level for C, H, N, O.

Table S1 Gibbs free energy of energy-minimized structures of **ox-NiPc-OH**.

ox-NiPc-OH	G (hartree)	ΔG (kcal/mol)
***cis*-isomer**	-2295.307470	0
***trans*-isomer**	-2295.296876	6.65

1.4. Reduction by GSH

1.4.1. Reduction of ox-NiPc-OH to NiPc by GSH

In a 50 mL test tube, GSH (2.1 g, 6.7 mmol) was completely dissolved in PBS (pH 5.8, 20 mL). Then, the solution of **ox-NiPc-OH** (1.0 g, 1.5 mmol) in acetone (20 mL) was added dropwise and stirred at room temperature for 24 h. The reaction mixture was centrifuged to remove the supernatant. After washing with water (30 mL × 3) and acetone (30 mL × 3), and the precipitate was dried under reduced pressure to give NiPc (0.83 g, 1.5 mmol, 98%).

1.4.2. Reduction of ox-NiPc-PEG to NiPc by GSH

In a 50 mL test tube, GSH (1.0 g, 3.3 mmol), **ox-NiPc-PEG** (0.15 g, 0.22 mmol), and water (10 mL) were stirred at room temperature for 3 d. The reaction mixture was centrifuged to remove the supernatant. After washing with water (30 mL × 5) and acetone (30 mL × 5), and the precipitate was dried under reduced pressure to obtain NiPc. NiPc was identified by MALDI-TOF mass spectrum (Fig. S5), IR absorption spectrum (Fig. S6), and elemental analysis (Table S1).

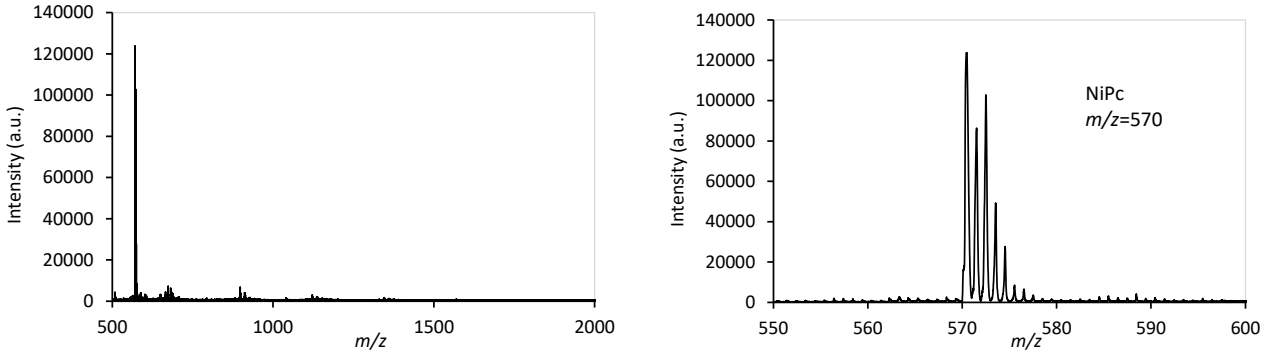

Fig. S5 MALDI-TOF mass spectrum of NiPc obtained from **ox-NiPc-PEG**. Matrix: dithranol.

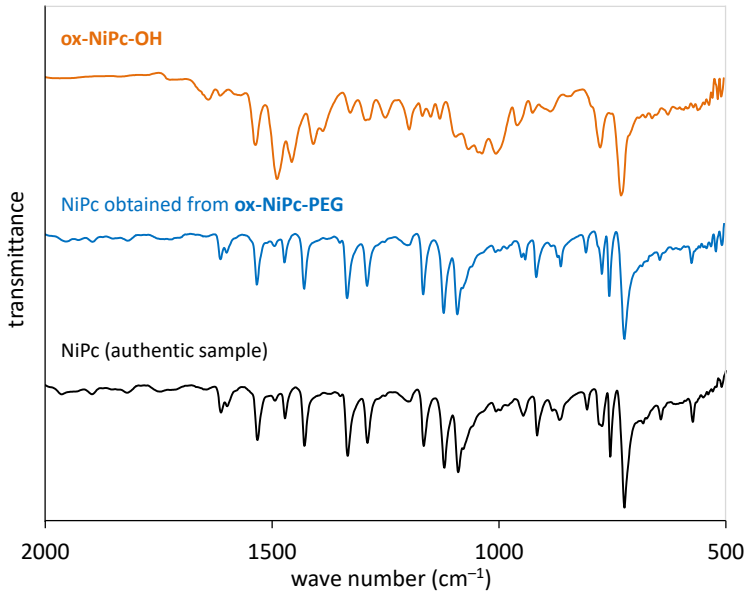

Fig. S6 IR spectra of **ox-NiPc-OH**, NiPc obtained from **ox-NiPc-PEG**, and NiPc[4] (authentic sample).

Table S2 Elemental analysis of NiPc obtained from **ox-NiPc-PEG**.

	H(%)	C(%)	N(%)
reduced product	2.83	67.10	19.81
calcd for NiPc	2.82	67.29	19.62

1.5. *In vitro* PA signal measurement

In 1.5 mL Eppendorf tubes, the PBS (pH 5.8) solution of 0.20–20 mM GSH (50 μL) or 0.20 mM amino acids (50 μL) were added to the 500 μM **ox-NiPc-PEG** solution (50 μL) and incubated at 37 °C for 30 min, respectively. After incubation, the PA signal intensities of these samples were measured under 680 nm pulsed laser irradiation (5 mJ/cm^2).

1.6. Detection of singlet oxygen

A water-soluble 9,10-anthracenedipropionic acid (ADPA) sodium salt was prepared according to the reported

procedure.[5] **ox-NiPc-PEG** (10 μM) was incubated with GSH (1 mM) in water for 24 h. A solution of ADPA sodium salt (0.10 mM) was added to the mixture in a quartz cuvette (optical path length: 10 mm). The mixture was photoirradiated using a Xenon light source device (MAX-303, Asahi Spectra Co., Ltd., Japan) equipped with VIS mirror module, rod lens (RLQL80-1, illuminance: 2.7 mW (λ = 680 nm) at the sample level), and long pass filter (λ > 590 nm). For positive control experiment, methylene blue (10 μM) was used instead of **ox-NiPc-PEG** and GSH. During photoirradiation, absorbance of ADPA at 400 nm were monitored every two minutes (Fig. S7).

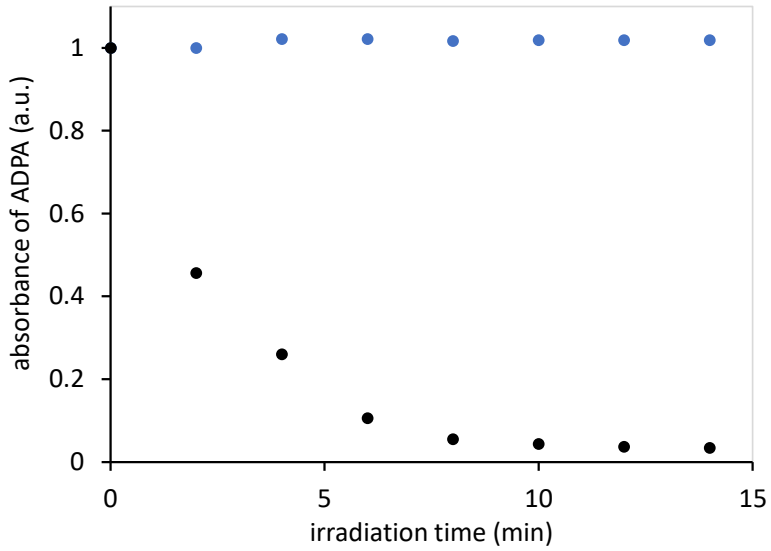

Fig. S7 Time-dependent change of absorbance of ADPA at 400 nm in H_2O in the presence of NiPc obtained from **ox-NiPc-PEG** under photoirradiation (blue). Methylene blue (black) was used as a positive control.

1.7. Cell experiment

1.7.1. Cell culture

The human lung carcinoma cell line, A549, was purchased from American Type Culture Collection (Manassas, VA). Normal cell line, Human Embryonic Kidney cells (HEK293), were purchased from Japanese Collection of Research Bioresources Cell Bank (JCRB Cell Bank), Japan. A549 cells and HEK293 cells were cultured in DMEM with 10% fetal vobine serum (FBS). Cells were cultured in a well-humidified incubator with 5% CO_2

and 95% air at 37 °C.

1.7.2. MTT cytotoxicity assay

The cell viability was evaluated by monitoring the reduction of MTT to formazan crystals using mitochondrial dehydrogenases. A549 cells were seeded into a 96-well microtiter plate at a density of 5×10^4 cells/well. The cells were incubated for 24 h for cell attachment. A549 cells were incubated at 37 °C for an additional 24 h with various concentrations of **ox-NiPc-PEG** (0, 0.010, 0.10, 1.0, 10, 50, and 100 μM). After washing the cells with PBS, MTT (0.20 mL, 0.5 mg/mL) was added to each well. After incubation at 37 °C for 4 h, the remaining MTT solution was removed, and the formazan crystals were dissolved in 200 μL of DMSO with gentle agitation for 5 min. The absorbance at 550 nm was measured using 800TS™ Absorbance Microplate Reader (BioTek Instruments, USA). For the evaluation of viability of HEK293, HEK293 cells were used instead of A549 cells. IC_{50} of **ox-NiPc-PEG** was over 100 μM (Fig. S8).

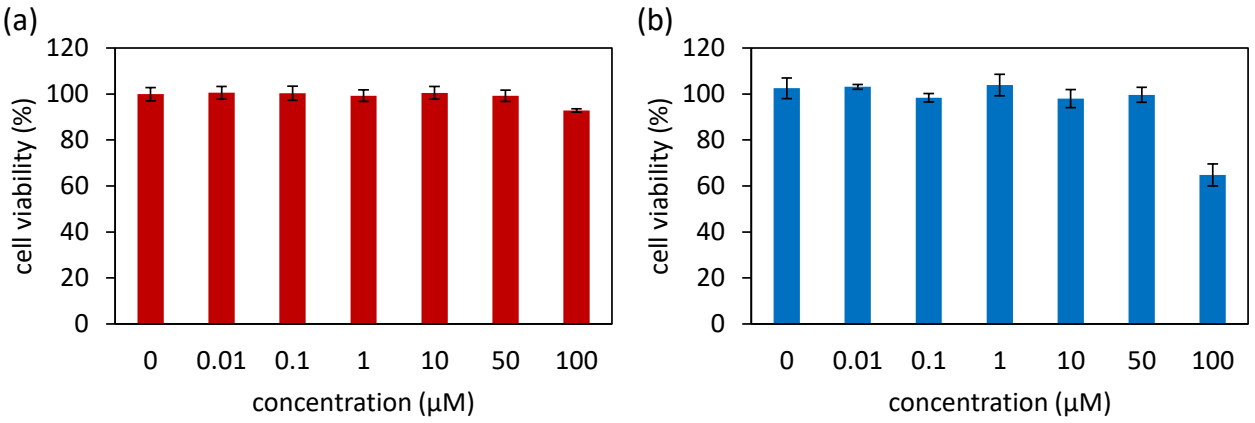

Fig. S8 Cell viabilities of (a) A549 and (b) HEK293 cells *in vitro* after incubation with **ox-NiPc-PEG** for 24 h. Mean values and standard deviation (n = 8).

1.7.3. PA signal increment caused by endogenous GSH

A549 and HEK293 cells were seeded into 12-well plates at a density of 1×10^5 cells/well and incubated at 37 °C for 24 h for cell attachment. For the thiol-trapping experiment, A549 cells were precultured with *N*-

ethylmaleimide (NEM, 2.0 mM) for 30 min. The aqueous solution of **ox-NiPc-PEG** was diluted with DMEM with 10% FBS and 1% P/S (final concentration: 10 μM). The cells were incubated with the **ox-NiPc-PEG** solution (1 mL) at 37 °C for 2 or 4 h. After incubation, the cells were washed with PBS and detached by trypsin/EDTA solution (0.10 mL). After adding PBS (0.90 mL), the cell suspension was transferred to 1.5 mL Eppendorf tube. After centrifugation, the supernatant was removed and PBS (1.0 mL) was added. The PA signal intensities were measured under 680 nm pulsed laser irradiation (5 mJ/cm^2).

1.8. *In vivo* experiment

1.8.1. A549 xenograft model

Female BALB/c mice in 9 weeks of age were purchased from Japan SLC, Inc., Japan. The mice were housed at the Institute of Laboratory Animals at Graduate School of Medicine of Kyoto University. All of animal experiments were approved by the Animal Research Committee of Kyoto University and carried out within its guidelines. To prepare the tumor-bearing mice, the injection of A549 cells (5×10^6 cells) in the right leg of each mouse was carried out.

1.8.2. *In vivo* PA signal intensity measurement

The A549 tumor-bearing mice were randomly divided into two groups (n = 4) (Fig. S9). For the first group, saline (30 mL) was pre-treated at the tumor site in the right leg and at the normal muscle in the left leg, respectively. After 30 min pretreatment, **ox-NiPc-PEG** (50 μM in 60 μL saline) was administered intratumorally in the right leg and subcutaneously in the left leg, respectively. For the second group, a pre-treatment of NEM (2.0 mM in 30 μL saline) was conducted in tumor sites before the intratumoral administration of **ox-NiPc-PEG** (50 μM in 60 μL saline). The PA tomography system was used to obtain from horizontal and vertical view images under pulsed laser irradiation (λ = 680 nm, 5 mJ/cm^2) (Fig. S10–S12). PA images of administrated sites were recorded before and post-injection at different time points (30 min, 3 h, and 6 h). The

PA intensities of regions of interest (ROI: muscle or tumor sites) were detected from each mouse in the same size (diameter of circle = 1.13 cm). The represent intensities were calculated in the mean of independent experiments (n = 4) with standard deviation (s.d.).

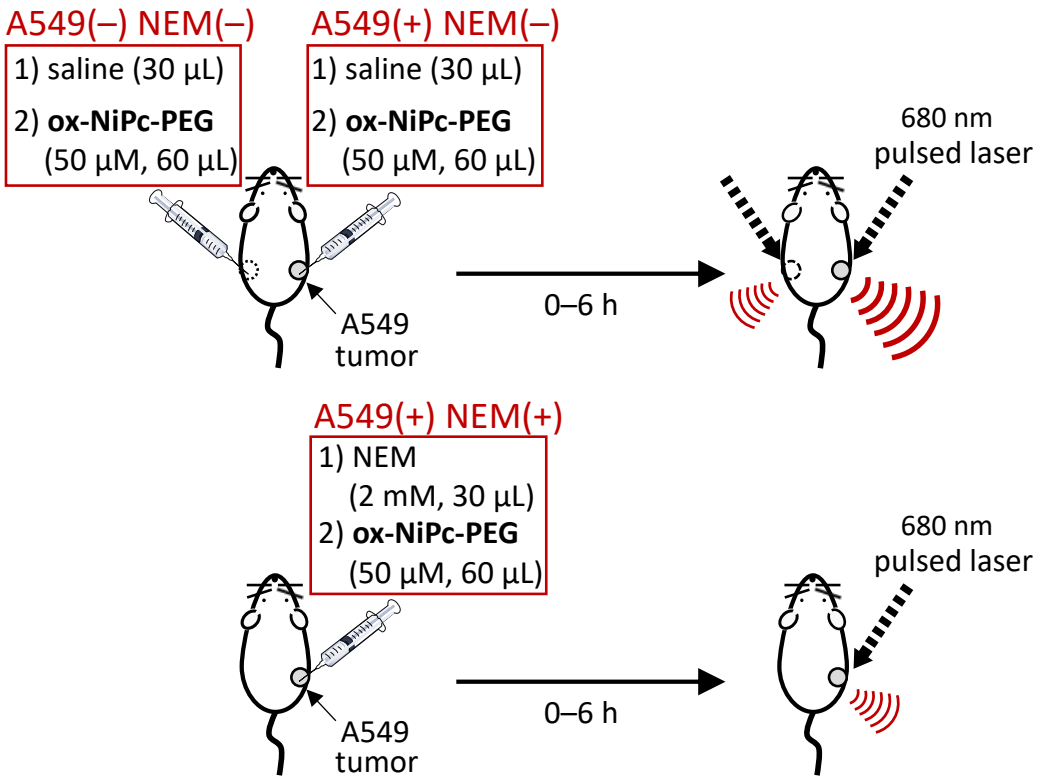

Fig. S9 Schematic illustration of *in vivo* experiment.

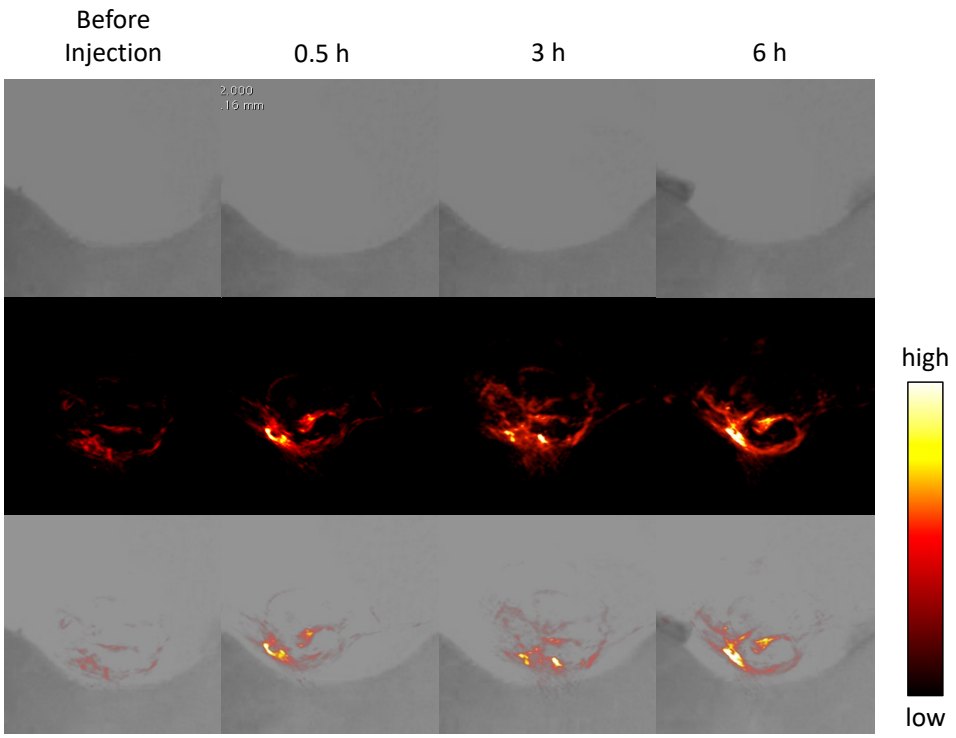

Fig. S10 *In vivo* PA side-view images of A549(+) NEM(–) region before and 0.5, 3, 6 h after injection (top: bright field, middle: PA image, bottom: merged).

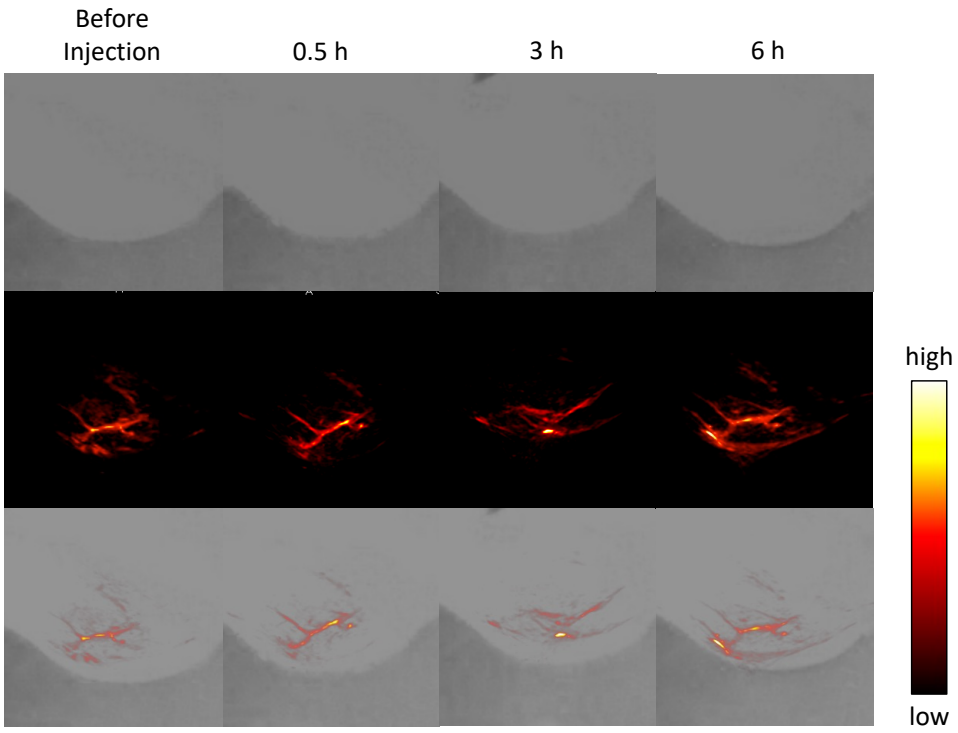

Fig. S11 *In vivo* PA side-view images of A549(–) NEM(–) region before and 0.5, 3, 6 h after injection (top: bright field, middle: PA image, bottom: merged).

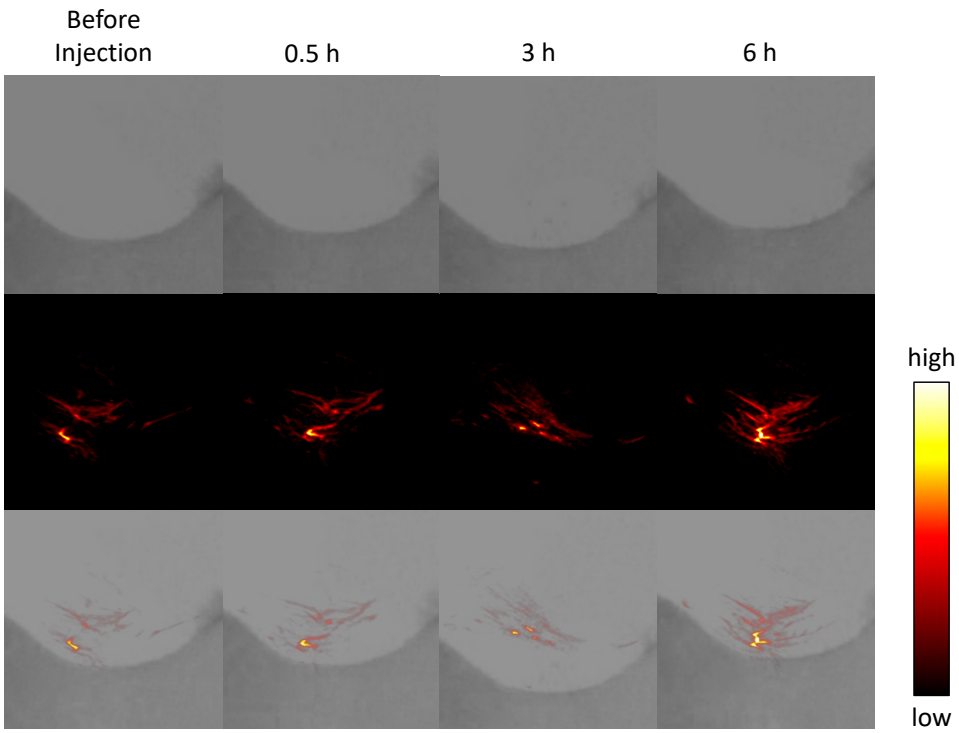

Fig. S12 *In vivo* PA side-view images of A549(+) NEM(+) region before and 0.5, 3, 6 h after injection (top: bright field, middle: PA image, bottom: merged).

2. X-ray crystallographic data

Single crystal of **ox-NiPc-OH** was obtained from recrystallization in CH_2Cl_2/hexane at room tempareture. Intensity data were collected on a RIGAKU Saturn 724 HG CCD system with VariMax Mo Optic using MoKα radiation. Crystal data are summarized in Table S3. The structures were solved by a direct method (SHELXT)[6] and refined by a full-matrix least square method on *F*2 for all reflections (SHELXL-2016).[7] All hydrogen atoms were placed using AFIX instructions, while all other atoms were refined anisotropically. The residual scattered electron densities, originating from disordered solvents, were eliminated by the SQUEEZE protocol equipped in PLATON.[8] The separation of the disorders on the hydroxyethoxy moiety is difficult, resulting in the Alerts B in the checkCIF/PLATON report. However, this problem does not affect the whole structure of the molecule. The molecular structure was visualized by Mercury.[9]

Table S3 Crystallographic data of **ox-NiPc-OH**.

CCDC number	2303413
Empirical formula	$C_{36}\ H_{26}\ N_8\ Ni\ O_4$
Formula weight	693.36
Temperature/K	143(2)
Crystal size/mm^3	0.1 × 0.1 × 0.1
Radiation	MoKα (λ = 0.71075)
Crystal color	red
Crystal system	orthorhombic
Space group	P b c n
a (Å)	12.655(3)
b (Å)	15.538(3)
c (Å)	17.066(3)
α (°)	90
β (°)	90
γ (°)	90
Volume (Å^3)	3355.7(12)
Z	4
D_{calc} (g/cm^3)	1.372
μ (mm^{-1})	0.63
F(000)	1432
2Θ range for data collection (°)	3.164 to 27.481
Index ranges	$-16 \le h \le 14, -20 \le k \le 19, -22 \le l \le 22$
Reflections collected	25539
Independent reflections	3849

Data/restraints/parameters	3849/0/223
Goodness-of-fit on F2	1.006
Final R indexes [I>=2σ (I)]	R1 = 0.0620, wR2 = 0.1136
Final R indexes [all data]	R1 = 0.0716, wR2 = 0.1177
Largest diff. peak/hole (e Å^{-3})	0.579/-0.56

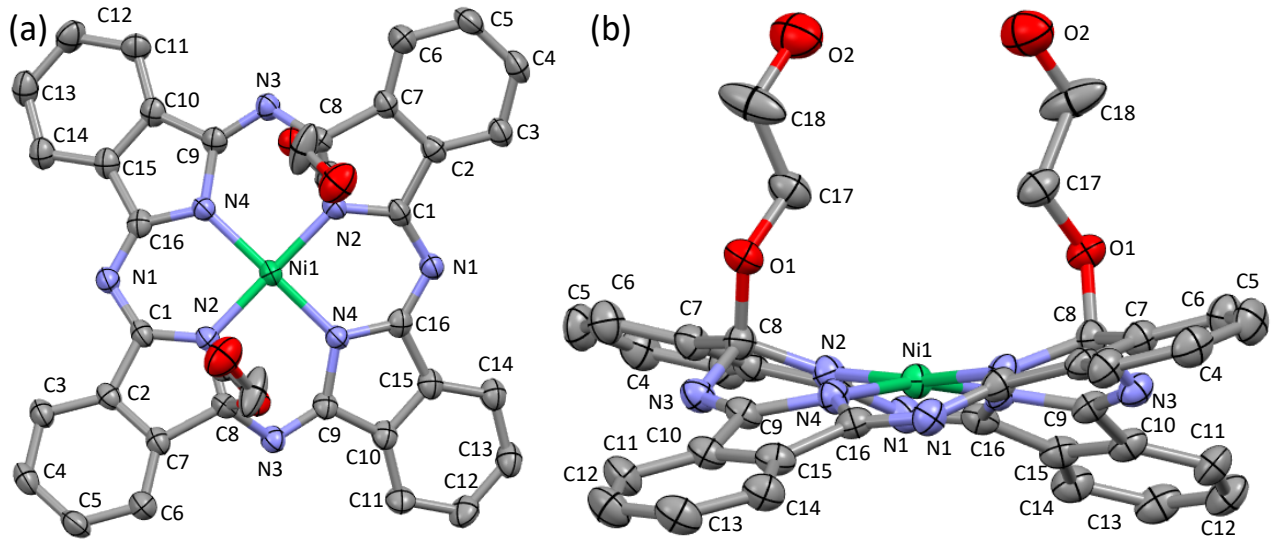

Fig. S13 (a) Top-view and (b) side-view of **ox-NiPc-OH** (50% ellipsoids) with labels. Hydrogen atoms and solvent molecules are omitted for clarity.

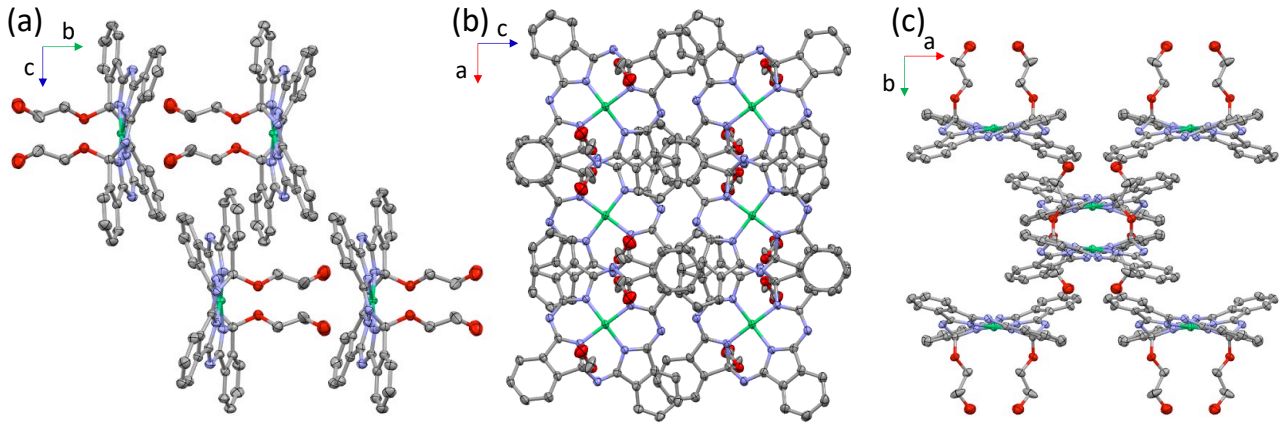

Fig. S14 Packing structure of **ox-NiPc-OH** (50% ellipsoids) viewed from the (a) *a* axis, (b) *b* axis, and (c) *c* axis.

Table S4 Selected (a) bond lengths and (b) angles for **ox-NiPc-OH**.

(a)	Length (Å)
Ni1—N2	1.845
Ni1—N4	1.871
O1—C8	1.434(4)
O1—C17	1.427(4)
N2—C1	1.328(4)
N2—C8	1.474(4)
N3—C8	1.448(4)
N3—C9	1.290(4)
N1—C1	1.352(4)
N1—C16	1.310(4)
N4—C16	1.365(4)
N4—C9	1.410(4)
O2—C18	1.393(6)
C1—C2	1.471(4)
C7—C2	1.377(4)
C7—C8	1.520(4)
C7—C6	1.378(5)
C15—C10	1.386(5)
C15—C16	1.473(5)
C10—C9	1.472(4)

(b)	Angle (deg)
N2—Ni1—N4	90.6
N2—Ni1—N4	90.3
C1—N2—C8	110.0(2)
C1—N1—C16	118.1(3)
C8—N3—C9	116.2(2)
C16—N4—C9	107.9(2)
N2—C1—N1	127.0(3)
N2—C1—C2	110.8(3)
O1—C8—N2	111.1(2)
O1—C8—N3	103.7(2)
O1—C8—C7	113.4(2)
N2—C8—N3	112.7(2)
N2—C8—C7	103.3(2)
N4—C16—C15	109.5(3)
N4—C16—N1	128.6(3)
N3—C9—N4	127.6(3)
N4—C9—C10	108.6(2)

3. NMR spectra

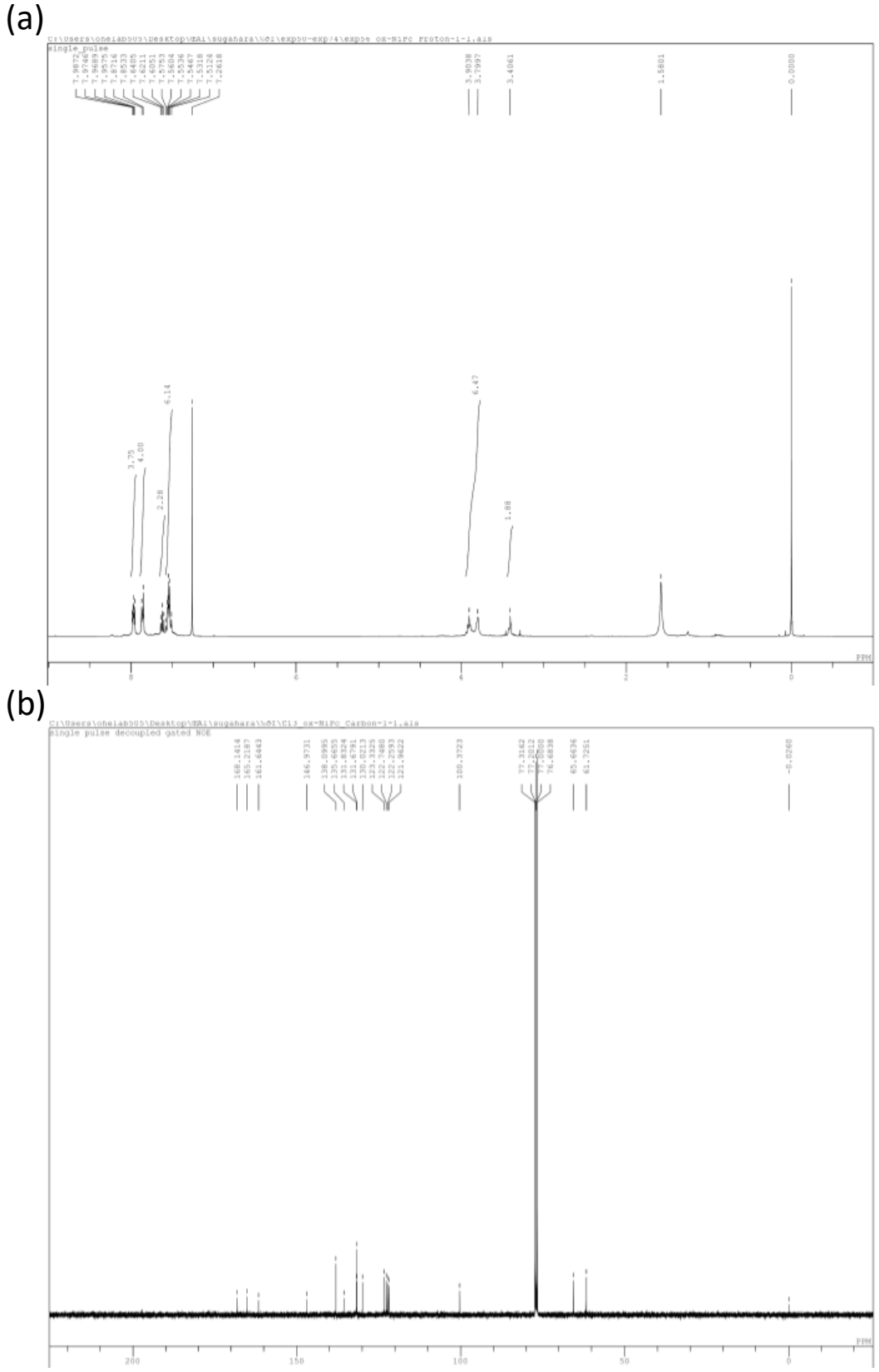

Fig. S15 (a) ^{1}H NMR and (b) ^{13}C NMR spectra of **ox-NiPc-OH** (400 MHz, $CDCl_3$, 25 °C).

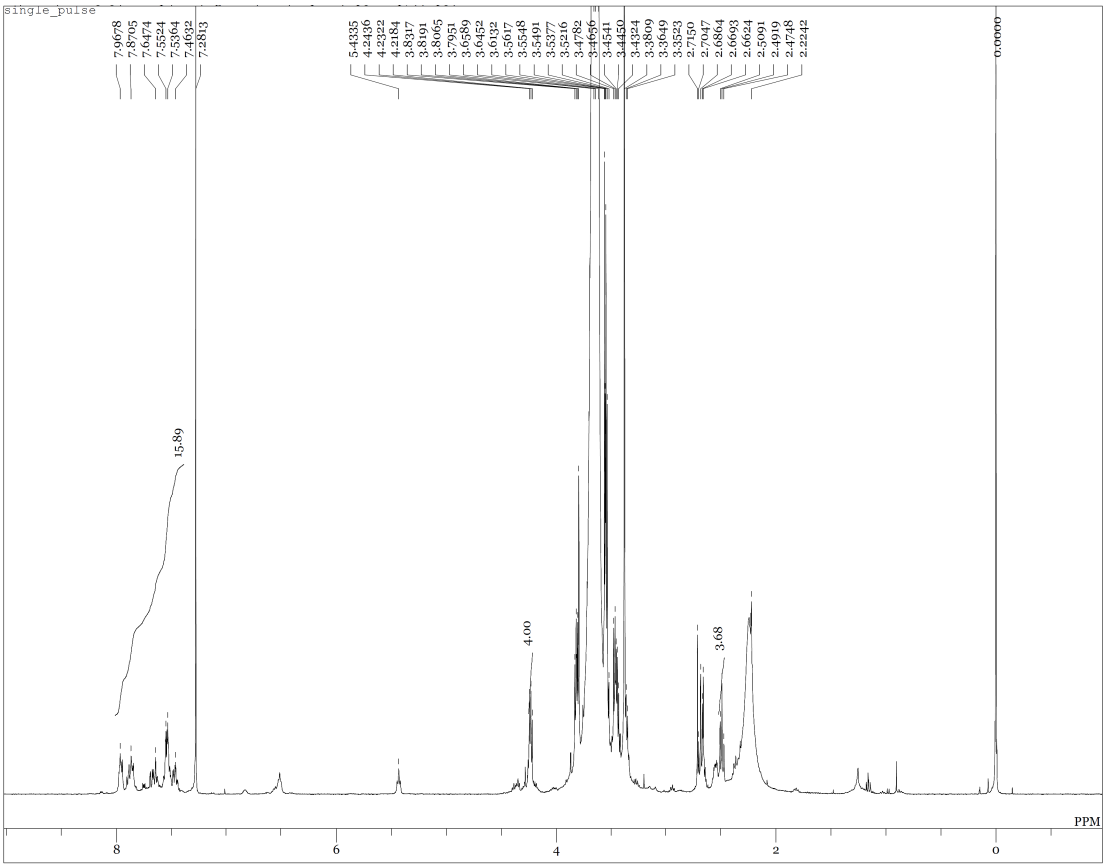

Fig. S16 ^{1}H NMR spectrum of **ox-NiPc-PEG** (400 MHz, $CDCl_3$, 25 °C).

4. Cartesian coordinates of energy-minimized structures

cis-isomer

Ni	-0.000000	-0.000000	0.359586
O	0.454115	2.604034	-1.600607
N	-0.766380	1.699958	0.246331
N	1.207937	3.134359	0.464721
N	-3.005218	1.242923	0.969480
N	1.718570	0.763356	0.585954
O	-0.644199	1.503251	-4.840079
H	-0.127602	1.249416	-5.613803
C	-2.014119	2.038921	0.524193
C	-1.008977	3.995045	-0.184695
C	-2.217928	3.480870	0.283450
C	-3.215205	5.642179	0.138432
H	-4.067493	6.304185	0.260286
C	-3.339796	4.285661	0.454773
H	-4.270000	3.866443	0.823556
C	3.839016	1.001525	1.484362
C	3.302996	2.287451	1.373837
C	0.000000	2.855925	-0.277489
C	2.809527	0.064898	0.989857
C	5.114652	0.785854	1.991248
H	5.518740	-0.217909	2.069136
C	5.846518	1.909511	2.392604
H	6.846492	1.782313	2.796918
C	4.026152	3.407785	1.759862
H	3.603538	4.402274	1.662514
C	1.958162	2.139819	0.770438
C	-2.001596	6.160342	-0.332571
H	-1.930267	7.218412	-0.568221
C	-0.878630	5.338183	-0.501492
H	0.064222	5.739035	-0.859596
C	-0.513388	2.301692	-2.604319
H	-1.133605	3.176722	-2.838322
H	-1.170427	1.482309	-2.289259
C	5.310126	3.199988	2.279043
H	5.902723	4.052170	2.599004
C	0.287104	1.874141	-3.826511
H	0.926177	2.709592	-4.148680
H	0.937940	1.032174	-3.557781
N	0.766380	-1.699958	0.246331
O	-0.454115	-2.604034	-1.600607
N	-1.207937	-3.134359	0.464721
N	3.005218	-1.242923	0.969480
N	-1.718570	-0.763356	0.585954
O	0.644199	-1.503251	-4.840079
H	0.127602	-1.249416	-5.613803
C	2.014119	-2.038921	0.524193
C	1.008977	-3.995045	-0.184695

C	2.217928	-3.480870	0.283450
C	3.215205	-5.642179	0.138432
H	4.067493	-6.304185	0.260286
C	3.339796	-4.285661	0.454773
H	4.270000	-3.866443	0.823556
C	-3.839016	-1.001525	1.484362
C	-3.302996	-2.287451	1.373837
C	-0.000000	-2.855925	-0.277489
C	-2.809527	-0.064898	0.989857
C	-5.114652	-0.785854	1.991248
H	-5.518740	0.217909	2.069136
C	-5.846518	-1.909511	2.392604
H	-6.846492	-1.782313	2.796918
C	-4.026152	-3.407785	1.759862
H	-3.603538	-4.402274	1.662514
C	-1.958162	-2.139819	0.770438
C	2.001596	-6.160342	-0.332571
H	1.930267	-7.218412	-0.568221
C	0.878630	-5.338183	-0.501492
H	-0.064222	-5.739035	-0.859596
C	0.513388	-2.301692	-2.604319
H	1.133605	-3.176722	-2.838322
H	1.170427	-1.482309	-2.289259
C	-5.310126	-3.199988	2.279043
H	-5.902723	-4.052170	2.599004
C	-0.287104	-1.874141	-3.826511
H	-0.926177	-2.709592	-4.148680
H	-0.937940	-1.032174	-3.557781

trans-isomer

C	-2.844975	2.849414	-0.595530
C	-3.659346	1.732723	-0.426382
C	-2.777828	0.594804	0.069815
N	-1.400770	1.108822	-0.124454
C	-1.458830	2.415612	-0.348307
C	2.982606	3.107373	0.531272
C	1.839632	3.860255	0.264724
C	0.759460	2.901673	-0.033657
N	1.229873	1.631378	0.038137
C	2.613769	1.688292	0.323895
N	-0.461549	3.313096	-0.314922
C	3.115700	-2.698635	0.906250
C	3.968638	-1.636086	0.633396
C	3.171539	-0.575801	-0.108949
N	1.755871	-1.032500	0.044486
C	1.770102	-2.295974	0.464092
N	3.481940	0.750960	0.330618
C	-2.575444	-3.020318	-0.761934
C	-1.464255	-3.769038	-0.369709
C	-0.423730	-2.802379	0.031887
N	-0.893284	-1.537192	-0.088675
C	-2.238965	-1.602328	-0.497730
N	-3.104828	-0.660422	-0.543273
N	0.768712	-3.190808	0.435263
C	3.571935	-3.869490	1.504163
C	4.927060	-3.932271	1.843186
C	5.785347	-2.857985	1.571583
C	5.316170	-1.693705	0.947580
C	4.188521	3.712174	0.860724
C	4.208795	5.110048	0.930622
C	3.058038	5.867298	0.664718
C	1.850384	5.249180	0.323295
C	-3.735570	-3.631526	-1.218757
C	-3.741794	-5.029986	-1.289586
C	-2.624697	-5.781695	-0.897047
C	-1.464046	-5.157689	-0.425660
C	-3.356328	4.084537	-0.976523
C	-4.733739	4.168583	-1.207409
C	-5.552848	3.042633	-1.061904
C	-5.023631	1.804599	-0.666701
Ni	0.173444	0.045587	-0.033915
O	3.594680	-0.729998	-1.464439
O	-2.868785	0.467994	1.498521
O	1.588084	-0.110257	-4.420905
C	2.140562	-0.912014	-3.384004
C	2.938015	0.026568	-2.485465
C	-3.891019	-0.105465	3.546218
O	-5.131700	-0.517291	4.104528
C	-4.109927	0.030100	2.046473
H	2.893304	-4.692785	1.700999
H	5.321583	-4.822955	2.323443
H	6.833414	-2.931638	1.847953
H	5.977478	-0.862955	0.725773
H	5.074276	3.116817	1.055534
H	5.131435	5.619778	1.192613
H	3.108699	6.950567	0.723942
H	0.953463	5.821098	0.110889
H	-4.598324	-3.041632	-1.510083
H	-4.627581	-5.543731	-1.651670
H	-2.663970	-6.865241	-0.959300
H	-0.594647	-5.726517	-0.113454
H	-2.700591	4.939861	-1.100491
H	-5.172440	5.113346	-1.514705
H	-6.616866	3.127808	-1.263653
H	-5.658369	0.929680	-0.574437
H	1.044575	-0.676097	-4.981591
H	1.362210	-1.407080	-2.786223
H	2.811775	-1.690361	-3.778603
H	3.710694	0.531472	-3.075541
H	2.272564	0.788648	-2.075342
H	-3.556093	0.861940	3.949852
H	-3.091154	-0.839045	3.728124
H	-5.013410	-0.611377	5.056964
H	-4.907656	0.760448	1.858461
H	-4.416604	-0.934282	1.626417

5. References

1. M. E. Ourailidou, P. Dockerty, M. Witte, G. J. Poelarends, F. J. Dekker, *Org. Biomol. Chem.* 2015, **13**, 3648–3653.
2. (a) A. D. Becke, *J. Chem. Phys.*, 1993, **98**, 5648–5652. (b) C. Lee, W. Yang, R. G. Parr, *Phys. Rev. B*, 1988, **37**, 785–789.
3. Gaussian 16, Revision B.01, M. J. Frisch, G. W. Trucks, H. B. Schlegel, G. E. Scuseria, M. A. Robb, J. R. Cheeseman, G. Scalmani, V. Barone, G. A. Petersson, H. Nakatsuji, X. Li, M. Caricato, A. V. Marenich, J. Bloino, B. G. Janesko, R. Gomperts, B. Mennucci, H. P. Hratchian, J. V. Ortiz, A. F. Izmaylov, J. L. Sonnenberg, D. Williams-Young, F. Ding, F. Lipparini, F. Egidi, J. Goings, B. Peng, A. Petrone, T. Henderson, D. Ranasinghe, V. G. Zakrzewski, J. Gao, N. Rega, G. Zheng, W. Liang, M. Hada, M. Ehara, K. Toyota, R. Fukuda, J. Hasegawa, M. Ishida, T. Nakajima, Y. Honda, O. Kitao, H. Nakai, T. Vreven, K. Throssell, J. A. Montgomery, Jr., J. E. Peralta, F. Ogliaro, M. J. Bearpark, J. J. Heyd, E. N. Brothers, K. N. Kudin, V. N. Staroverov, T. A. Keith, R. Kobayashi, J. Normand, K. Raghavachari, A. P. Rendell, J. C. Burant, S. S. Iyengar, J. Tomasi, M. Cossi, J. M. Millam, M. Klene, C. Adamo, R. Cammi, J. W. Ochterski, R. L. Martin, K. Morokuma, O. Farkas, J. B. Foresman, and D. J. Fox, Gaussian, Inc., Wallingford CT, 2016.
4. H. Tomoda, S. Saito, S. Shiraishi, *Chem. Lett.* 1983, **12**, 313–316.
5. B. A. Lindig, M. A. J. Rodgers, A. P. Schaap, *J. Am. Chem. Soc.* 1980, **102**, 5590–5593.
6. Sheldrick, G. M. SHELXT – Integrated Space-Group and Crystal-Structure Determination. *Acta Crystallogr. Sect. A* 2015, **71**, 3–8.
7. Sheldrick, G. M. Crystal Structure Refinement with SHELXL. *Acta Crystallogr. Sect. C* 2015, **71**, 3–8.
8. Spek, A. L. PLATON SQUEEZE: A Tool for the Calculation of the Disordered Solvent Contribution to the Calculated Structure Factors. *Acta Crystallogr. Sect. C* 2015, **71**, 9–18.
9. Provided by The Cambridge Crystallographic Data Centre (CCDC): https://www.ccdc.cam.ac.uk/solutions/csd-system/components/mercury/